33

Nonlinear Bifurcation Analysis

TABLE OF CONTENTS

		Page
§33.1	**Introduction**	33–3
§33.2	**Bifurcation Analysis Levels**	33–3
§33.3	**Recapitulation of Governing Equations**	33–3
§33.3.1	Residual Equilibrium Equations	33–4
§33.3.2	Rate Equations	33–4
§33.3.3	Stiffness and Load Rates	33–5
§33.3.4	Limitations of λ-Parametrized Forms	33–5
§33.4	**Branching Analysis Preliminaries**	33–5
§33.4.1	State Decomposition in the Active Subspace	33–6
§33.4.2	Failure of First-Order Rate Equations at Bifurcation	33–6
§33.5	**Simple Bifurcation Analysis**	33–7
§33.5.1	State Decomposition	33–7
§33.5.2	Finding σ	33–7
§33.5.3	Special Quadratic Equation Cases	33–9
§33.5.4	Are the Roots Always Real?	33–10
§33.6	**Multiple Bifurcation Points**	33–10
§33.7	**The Hinged Rigid Cantilever**	33–11
§33.7.1	Finding the Critical Point	33–11
§33.7.2	Branching Analysis	33–12
§33.8	**The Inclined Spring Propped Rigid Cantilever**	33–13
§33.8.1	Critical Point Analysis	33–13
§33.8.2	Stiffness Analysis	33–15
§33.	**Exercises**	33–16
§33.	**Solutions to Exercises**	33–17

§33.1. Introduction

The study of stability of conservative systems was started in Chapters 28-29 by using the simplified model of linearized prebuckling (LPB), in which geometric changes prior to buckling are neglected. This was followed in Chapter 29 by a qualitative study of the more general case. This study classified *simple* (isolated) critical points into four types: limit point, asymmetric bifurcation, stable-symmetric bifurcation, and unstable-symmetric bifurcation. This classification is especially helpful in understanding the effect of imperfections on stability, as covered in the next Chapter.

This Chapter presents a more detailed mathematical study of bifurcation of geometrically nonlinear conservative systems by studying the behavior of *equilibrium branches* in the vicinity of a simple bifurcation point.[1] The study is subsumed under the title of *nonlinear bifurcation* to emphasize that we are dealing with the general case as opposed to the LPB model. A simple one-DOF example is worked out to illustrate the analysis procedure.

§33.2. Bifurcation Analysis Levels

Nonlinear bifurcation analysis can be carried out at several forward coupled levels, as required by application needs.[2] Four levels of increasing detail are schematized in Figure 33.1, which assumes the occurrence of a simple (isolated) bifurcation point at B. Levels are forwardly coupled; for example doing level 3 requires information from levels 1 and 2.

1. *Locate*: find where B occurs while tracing a response. Can be done by watching changes of sign of the determinant of $\mathbf{K}$ or, equivalently, monitoring the sign of pivots in a $\mathbf{K} = \mathbf{L}\,\mathbf{D}\mathbf{L}^T$ factorization. For the latter method see Remark **?**.
2. *Determine subspace*: having located B, determine vectors $\mathbf{y}$ (particular solution) and $\mathbf{z}$ (null eigenvector for simple bifurcation). Together they form a state subspace "where the action is." Requires a partial eigensolution of $\mathbf{K}$; more precisely the determination of $\mathbf{z}$ at B.
3. *Branching analysis*: having located B, and gotten $\mathbf{y}$ and $\mathbf{z}$, find the directions $\dot{\mathbf{u}}_1$ and $\dot{\mathbf{u}}_2$ of tangents to the equilibrium paths (branches) that pass through B. These tangents lie in the ($\mathbf{y}$, $\mathbf{z}$) subspace, but are not necessarily aligned with those vectors. Requires an analysis of the second order rate equations $\ddot{\mathbf{r}} = \mathbf{0}$.
4. *Branch curvature analysis*: having located B and determined $\mathbf{y}$, $\mathbf{z}$, $\dot{\mathbf{u}}_1$ and $\dot{\mathbf{u}}_2$, find the curvatures of the equilibrium paths (branches) passing through B. Requires an analysis of the third order equation $\dddot{\mathbf{r}} = \mathbf{0}$.

The information necessary for level 3 is difficult to extract from a general purpose nonlinear FEM program because it requires stiffness and incremental load pseudotime rates. That needed for level 4 is truly inaccessible. For this reason most commercial FEM programs provide only levels 1 and 2 on a routine basis. In the present Chapter we study up to level 3 (branching analysis) for simple examples that can be entirely worked out either by hand, or through a computer algebra system (CAS). The practical difficulties of implementing level 3 and beyond for more complicated cases should be kept in mind.

---

[1] This technique and related ones are collectively known as *perturbation analysis* in applied mathematics.

[2] For example, in preliminary design only the location of the bifurcation point closest to the reference configuration would be of interest to set up a safety factor.

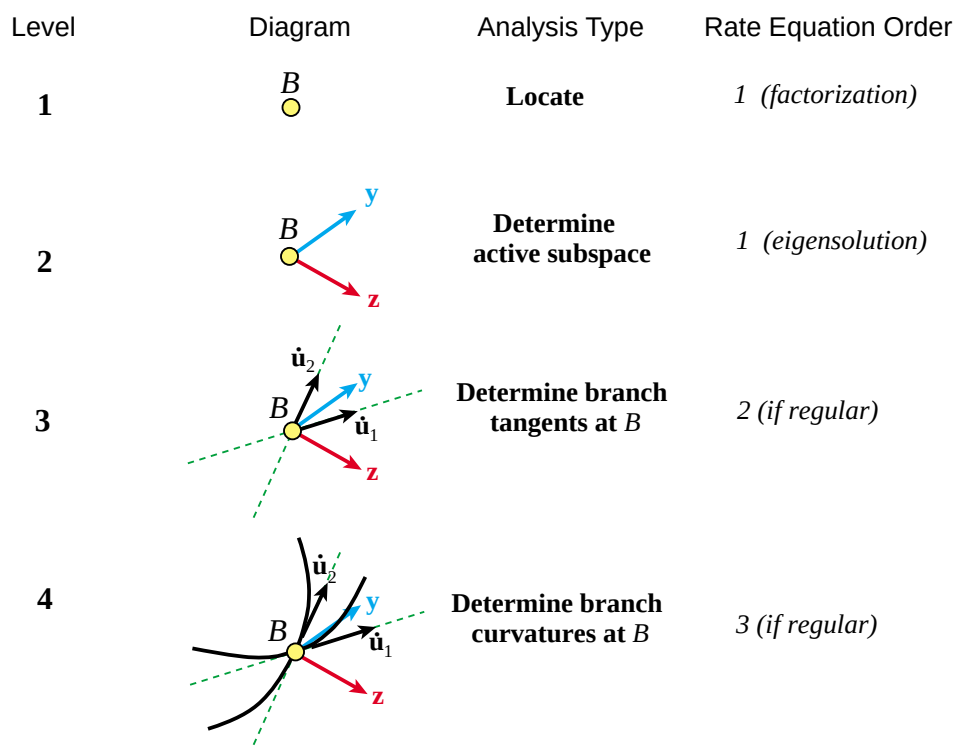

FIGURE 33.1. The four levels of information in nonlinear buckling analysis. They are shown for a *simple* (isolated) bifurcation point in 3D ($\dot{\mathbf{u}}_1$, $\dot{\mathbf{u}}_2$, λ) space, with λ (not pictured) normal to the (**y**, **z**) plane.

§33.3. Recapitulation of Governing Equations

Below we recall discrete governing equations derived in Chapters 3–4, and introduce additional nomenclature required for the branching analysis carried out in §33.4 and §33.5.

§33.3.1. Residual Equilibrium Equations

The one-parameter, total-residual equilibrium equations are

$$\mathbf{r}(\mathbf{u}, \lambda) = \mathbf{0}, \tag{33.1}$$

where λ is the stage control parameter and $\mathbf{u}$ is the state vector. Solutions of this equation may be conveniently represented in parametric form as

$$\mathbf{u} = \mathbf{u}(t), \qquad \lambda = \lambda(t), \tag{33.2}$$

in which t is a dimensionless pseudotime parameter. Two important special choices for t are

$$t = \lambda, \qquad t = s, \tag{33.3}$$

These lead to the λ-*parametrized* and *arclength* forms, respectively. In the analysis of **?**, however, t is kept arbitrary.

§33.3.2. Rate Equations

Rate equations are systems of ordinary differential equations obtained by successive differentiation of (33.1) with respect to t. Recall that $\mathbf{K}$ and $\mathbf{q}$ denote the tangent stiffness matrix and incremental load vector, respectively, given by the residual gradients

$$\mathbf{K} = \frac{\partial \mathbf{r}}{\partial \mathbf{u}}, \qquad \mathbf{q} = -\frac{\partial \mathbf{r}}{\partial \lambda}. \tag{33.4}$$

Their entries are given by $K_{ij} = \partial r_i/\partial u_j$ and $q_i = -\partial r_i/\partial\lambda$, respectively. Using superposed dots to denote t-differentiation we obtain

$$\dot{\mathbf{r}} = \mathbf{K}\dot{\mathbf{u}} - \mathbf{q}\dot{\lambda} = \mathbf{0}, \tag{33.5}$$

$$\ddot{\mathbf{r}} = \mathbf{K}\ddot{\mathbf{u}} + \dot{\mathbf{K}}\dot{\mathbf{u}} - \dot{\mathbf{q}}\dot{\lambda} - \mathbf{q}\ddot{\lambda} = \mathbf{0}, \tag{33.6}$$

$$\dddot{\mathbf{r}} = \mathbf{K}\dddot{\mathbf{u}} + \dot{\mathbf{K}}\ddot{\mathbf{u}} + \ddot{\mathbf{K}}\dot{\mathbf{u}} - \mathbf{q}\dddot{\lambda} - \dot{\mathbf{q}}\ddot{\lambda} - \ddot{\mathbf{q}}\dot{\lambda} = \mathbf{0}. \tag{33.7}$$

Eq. (33.5) is a system of first-order rate equations, also called the *incremental stiffness equations* or simply the *stiffness equations*. Eq. (33.6) is a system of second-order rate equations, also called the *stiffness rate equations*. Eq. (33.7) is a system of third-order rate equations. And so on. For the branching analysis undertaken in §33.5 we will need to go up to (33.6).

§33.3.3. Stiffness and Load Rates

In the study of the second-order equations (33.6) the stiffness matrix rate $\dot{\mathbf{K}}$ and incremental load vector rate $\dot{\mathbf{q}}$ may be conveniently expressed as linear combinations of $\dot{\mathbf{u}}$ and $\dot{\lambda}$:

$$\dot{\mathbf{K}} = \mathbf{L}\,\dot{\mathbf{u}} + \mathbf{N}\,\dot{\lambda}, \qquad \dot{\mathbf{q}} = -\mathbf{N}\,\dot{\mathbf{u}} + \mathbf{h}\,\dot{\lambda}. \tag{33.8}$$

The entries of these newly defined matrices and vectors are given by

$$L_{ijk} = \frac{\partial^2 r_i}{\partial u_j \partial u_k} = \frac{\partial K_{ij}}{\partial u_k}, \quad N_{ij} = \frac{\partial^2 r_i}{\partial u_j \partial \lambda} = \frac{\partial K_{ij}}{\partial \lambda} = -\frac{\partial q_i}{\partial u_j}, \quad h_i = -\frac{\partial^2 r_i}{\partial \lambda \partial \lambda} = \frac{\partial q_i}{\partial \lambda}. \tag{33.9}$$

Remark 33.1. Note that $\mathbf{L}$ is a three-dimensional array that may be called a *cubic matrix* to distinguish it from an ordinary matrix. (May be also interpreted as a third order tensor.) Postmultiplying a cubic matrix by a vector yields an ordinary matrix. For example $\mathbf{L}\,\dot{\mathbf{u}}$ is a matrix.

§33.3.4. Limitations of λ-Parametrized Forms

If one chooses $t = \lambda$, the rate equations simplify because $\dot{\lambda} = 1$ and $\ddot{\lambda} = \dddot{\lambda} = 0$. Using primes to denote differentiation with respect to λ, the first two rate forms (33.5) and (33.6) reduce to

$$\mathbf{K}\,\mathbf{u}' - \mathbf{q} = \mathbf{0}, \tag{33.10}$$

$$\mathbf{K}\,\mathbf{u}'' + \mathbf{K}'\,\mathbf{u}' - \mathbf{q}' = \mathbf{0}, \tag{33.11}$$

in which

$$\mathbf{K}' = \mathbf{L}\,\mathbf{u}' + \mathbf{N}, \qquad \mathbf{q}' = -(\mathbf{N}\,\mathbf{u}' + \mathbf{h}). \tag{33.12}$$

These are unsuitable, however, in the vicinity of a bifurcation point, because the relation between $\mathbf{u}$ and λ ceases to be unique, and the more general parametrized forms (33.5)–(33.7) must be used.

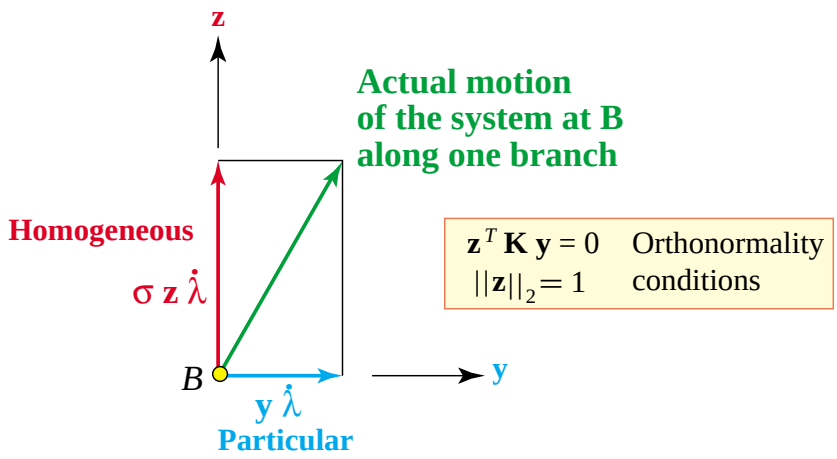

FIGURE 33.2. State decomposition at simple (isolated) bifurcation point B, depicted on the (**y**, **z**) plane.

§33.4. Branching Analysis Preliminaries

At a simple critical point, say B, $\mathbf{K}$ becomes once singular. Therefore it possesses one null right eigenvector, which as usual will be denoted by $\mathbf{z}$. This eigenvector will be *normalized to unit length*. As discussed in Chapter 5, if the eigenvector is orthogonal to the incremental load vector $\mathbf{q}$, so that $\mathbf{q}^T\,\mathbf{z} = 0$, the critical point is a bifurcation point, whreas if $\mathbf{q}^T\,\mathbf{z} \neq 0$, it is a limit point. The ensuing analysis assumes that B is an *isolated bifurcation point*.

§33.4.1. State Decomposition in the Active Subspace

The conditions for bifurcation may be summarily restated as

$$\boxed{\mathbf{K}\,\mathbf{z} = \mathbf{0}, \qquad \|\mathbf{z}\|_2^2 = \mathbf{z}^T\mathbf{z} = 1, \qquad \mathbf{q}^T\mathbf{z} = 0.} \tag{33.13}$$

where subscripts B as well as cr are omitted to reduce clutter. Since the system is assumed to be conservative, $\mathbf{K}$ is symmetric. Thus $\mathbf{z}$ is also a left eigenvector of $\mathbf{K} = \mathbf{K}^T$. In structural mechanics $\mathbf{z}$ is called a *buckling mode shape*. This name conveys the idea that the structure "jumps" from the prebuckling configuration into the buckled shape. Although the scenario is correct for the LPB model, we shall see that it is not necessarily appropriate in the general case.

At the bifurcation point B the state vector $\mathbf{u}$ and control parameter λ assume values $\mathbf{u}_B$ and λ_B, respectively. We will study *small* deviations of $\mathbf{u}$ and λ in the neighborhood of B. These deviations are denoted by $\Delta\mathbf{u} = \mathbf{u} - \mathbf{u}_B$ and $\Delta\lambda = \lambda - \lambda_B$, respectively. For small deviations from the bifurcation point the relation between $\Delta\mathbf{u}$ and $\Delta\lambda$ may be linearized as

$$\Delta\mathbf{u} = (\sigma\,\mathbf{z} + \mathbf{y})\,\Delta\lambda, \tag{33.14}$$

where $\mathbf{y}$ is the *particular solution* introduced in §31.4.2, and σ is the *buckling mode amplitude*. The use of σ is necessary since the normalized $\mathbf{z}$ has unit length.

Dividing by Δt and passing to the limit $\Delta t \to 0$, we obtain the rate form of the above equation:

$$\dot{\mathbf{u}} = (\sigma\,\mathbf{z} + \mathbf{y})\,\dot{\lambda}. \tag{33.15}$$

This decomposition of $\dot{\mathbf{u}}$ in the $\mathbf{y}$, $\mathbf{z}$ plane is depicted in Figure 33.2, which is a duplicate of Figure **?**. The key difference is that the prebuckling geometric restrictions of LPB no longer apply.

§33.4.2. Failure of First-Order Rate Equations at Bifurcation

To carry out a level-3 branching analysis, we will assume that information from levels 1 and 2 is available. Hence the location of B, as well as vectors $\mathbf{y}$ and $\mathbf{z}$, are on hand. The additional information sought at this level are the tangents to the equilibrium branches passing through B, as pictured in Level 3 of Figure 33.1. Now the tangent to each branch is determined by the linearized rate form (33.15), which in turn is fully defined if σ is known. So the level 3 key goal is: find σ.

Can the first-order rate equations (33.5) provide σ? No. This is worked out in Exercise 33.3, which shows that the result is indeterminate: $\sigma = 0/0$. To get a deterministic result it is necessary to use information from *higher-order rate equations*. This is covered in the following section. We shall see that the second-order rate equations (33.6) are usually sufficient.

§33.5. Simple Bifurcation Analysis

The ensuing analysis assumes that the rank deficiency of $\mathbf{K}$ at bifurcation is only one. Thus $\mathbf{z}$ is the only null eigenvector. This is called a *simple, isolated* or *distinct* bifurcation point. Under certain regularity conditions noted later, we shall see that at such points there can be at most *two* equilibrium paths that pass through B. Such paths are called *branches*.

§33.5.1. State Decomposition

As previously stipulated, assume that we have located a bifurcation point B and computed the null eigenvector $\mathbf{z}$. Our next task is to examine the structural behavior in the *neighborhood* of B. This analysis is important to answer questions pertaining to the *safety* of the structure and its sensitivity to imperfections. From §33.4.1 we know that the state rate $\dot{\mathbf{u}}$ at B can be decomposed as per (33.15). In that decomposition the particular solution vector $\mathbf{y}$ solves the system

$$\mathbf{K}\,\mathbf{y} = \mathbf{q}, \qquad \mathbf{z}^T\,\mathbf{K}\,\mathbf{y} = 0, \tag{33.16}$$

which is simply the first-order incremental equation augmented by an orthonormality constraint. Imposing this constraint removes the singularity (rank deficiency) of $\mathbf{K}$ at B. Note that $\mathbf{y}$ would be aligned along the incremental velocity vector $\mathbf{v} = \mathbf{K}^{-1}\,\mathbf{q}$ at B if $\mathbf{K}$ were nonsingular.

Remark 33.2. The homogeneous solution $\mathbf{z}$ lies in the null space of $\mathbf{K}$ whereas the particular solution $\mathbf{y}$ lies in the range space of $\mathbf{K}$. In more physical terms we may say that $\mathbf{y}$ "responds" to the load (the incremental load vector $\mathbf{q}$) whereas $\mathbf{z}$, like any homogeneous solution, is dictated by the boundary conditions.

Remark 33.3. In some respects the state decomposition (33.15) is analogous to the decomposition of element motions into purely-deformational and rigid-body, studied for the corotational kinematic description. Here $\mathbf{z}$ takes up the role of rigid body mode. The decomposition (33.15) is, however, expressed in terms of rates because it is *local*: it is restricted to the vicinity of the bifurcation point.

§33.5.2. Finding σ

The level 3 information on the equilibrium branches at B involves their *tangents* at B. Because $\mathbf{y}$ and $\mathbf{z}$ are on hand from levels 1 and 2, those tangents are determined if in addition we know σ, since (33.15) provides the tangent directions $(\dot{\lambda}, \dot{\mathbf{u}})$ in the $(\lambda, \mathbf{u})$ control-state space.

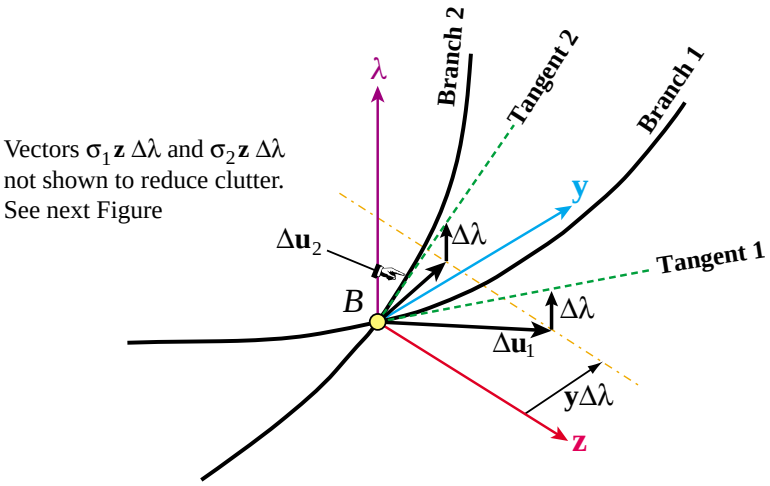

FIGURE 33.3. Intersection of two equilibrium paths at an simple (isolated) bifurcation point B, depicted in the $(\lambda, \mathbf{y}, \mathbf{z})$ subspace of the control-state space.

It was noted in §33.4.2 the first-order rate equations (33.5) cannot provide σ. It is necessary to go to the second-order rate equations (33.6), which are repeated here for convenience:

$$\boxed{\mathbf{K}\,\ddot{\mathbf{u}} + \dot{\mathbf{K}}\,\dot{\mathbf{u}} - \mathbf{q}\,\ddot{\lambda} - \dot{\mathbf{q}}\,\dot{\lambda} = \mathbf{0}.} \tag{33.17}$$

Premultiplying both sides[3] by $\mathbf{z}^T$ and taking account of the bifurcation conditions $\mathbf{Kz} = \mathbf{0}$ (whence $\mathbf{z}^T\mathbf{K} = \mathbf{0}$ because $\mathbf{K} = \mathbf{K}^T$) and $\mathbf{q}^T\mathbf{z} = \mathbf{z}^T\mathbf{q} = 0$, we get at B the *scalar* equation

$$\boxed{\mathbf{z}^T\dot{\mathbf{K}}\,\dot{\mathbf{u}} - \mathbf{z}^T\,\dot{\mathbf{q}}\dot{\lambda} = 0.} \tag{33.18}$$

Replacing $\dot{\mathbf{K}}$ and $\dot{\mathbf{q}}$ by the expressions (33.8) gives

$$\mathbf{z}^T(\mathbf{L}\,\dot{\mathbf{u}} + \mathbf{N}\,\dot{\lambda})\dot{\mathbf{u}} + \mathbf{z}^T(\mathbf{N}\,\dot{\mathbf{u}} + \mathbf{h}\,\dot{\lambda})\,\dot{\lambda} = 0. \tag{33.19}$$

Finally, inserting the state decomposition NFEM:Ch33:eqn:StateDecompositionInRateForm of $\dot{\mathbf{u}}$ yields

$$\boxed{\mathbf{z}^T\left[\mathbf{L}\,(\mathbf{y} + \sigma\,\mathbf{z})\,\dot{\lambda} + \mathbf{N}\,\dot{\lambda}\right]\,(\mathbf{y} + \sigma\mathbf{z})\,\dot{\lambda} + \mathbf{z}^T\,\left[\mathbf{N}\,(\mathbf{y} + \sigma\,\mathbf{z})\dot{\lambda} + \mathbf{h}\,\dot{\lambda}\right]\,\dot{\lambda} = 0.} \tag{33.20}$$

Removing the common differential factor $(\dot{\lambda})^2$ and collecting terms in σ we arrive at the quadratic equation

$$\boxed{a\sigma^2 + 2b\sigma + c = 0,} \tag{33.21}$$

in which

$$\boxed{a = \mathbf{z}^T\mathbf{L}\mathbf{z}\mathbf{z}, \quad b = \mathbf{z}^T\,[\mathbf{L}\mathbf{z}\mathbf{y} + \mathbf{L}\mathbf{y}\mathbf{z} + 2\mathbf{N}\mathbf{z}]\,, \quad c = \mathbf{z}^T\,[\mathbf{L}\mathbf{y}\mathbf{y} + 2\mathbf{N}\mathbf{y} + \mathbf{h}]\,.} \tag{33.22}$$

[3] This dot-product operation is called a *projection* of the second-order rate equations (33.6) onto the null space of $\mathbf{K}$.

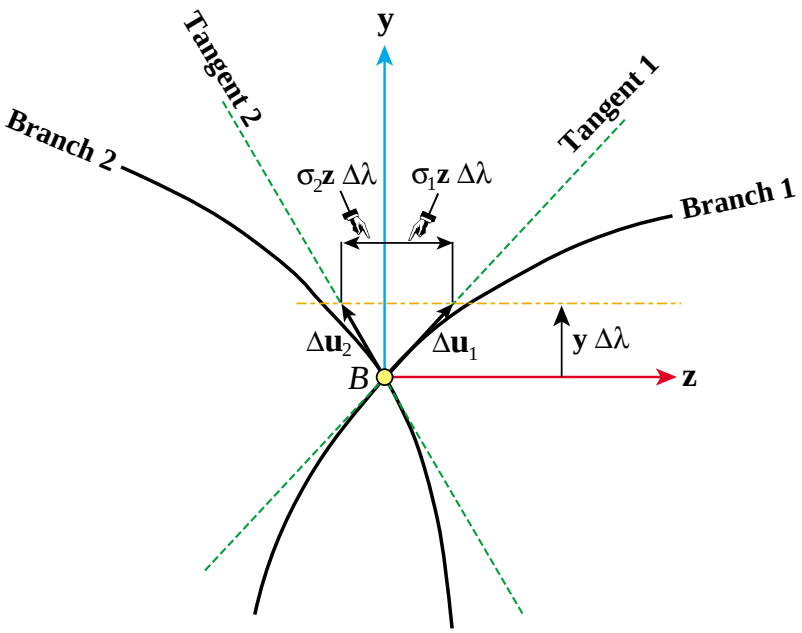

FIGURE 33.4. Same as Figure 33.3 but looking down the λ axis onto the (**y**, **z**) plane.

This quadratic equation generally provides two roots: σ_1 and σ_2. In what follows we shall assume that these two roots are real (see §33.5.4 below).

Substitution of σ_1 and σ_2 into (31.16) furnishes the *branching directions* at the bifurcation point:

$$\dot{\mathbf{u}}_1 = (\mathbf{y} + \sigma_1\,\mathbf{z})\,\dot{\lambda}, \qquad \dot{\mathbf{u}}_2 = (\mathbf{y} + \sigma_2\,\mathbf{z})\,\dot{\lambda}. \tag{33.23}$$

These are sketched in Figure 33.3 in the three-dimensional space (**y**, **z**, λ) with origin at B. Figure 33.4 projects this picture onto the (**y**, **z**) plane for additional clarity.

The key result of this subsection is that *there are at most two branches emanating from a simple bifurcation point.* The classification of such points into asymmetric and symmetric bifurcation points according to the values of σ_1 and σ_2 appears in the Exercises. In §33.7 an illustrative example is worked out by hand.

§33.5.3. Special Quadratic Equation Cases

Consider the quadratic equation (33.21). If $a = 0$ one root, say σ_2, becomes infinite while the other, assuming $b \neq 0$, is $\sigma_1 = -c/(2b)$. Then $\dot{\mathbf{u}}_2$ becomes aligned with **z**. Only in this case it is justified to call **z** the "buckling mode." This particular case, which is quite common in Civil Engineering structures, leads to the so-called *symmetric* bifurcation — see Exercise 33.2.

If $a = b = c = 0$ the second-order rate equations (33.6) do not provide any local information as regards branches at B. Then one must continue to the third order rate form (33.7). This will give a cubic equation in σ with four real coefficients. Since such an equation can have one or three real roots, things get far more complicated. If all four coefficients vanish, one must go to the fourth-order rate form, and so on. (For a mathematician specialized in this kind of perturbation analysis, hell is a place where the first one thousand rate forms yield no information.)

The case $a = b = 0, c \neq 0$ automatically leads to complex roots as one takes the limits $a \to 0$ and $b \to 0$, because $b^2 - ac < 0$, so it is excluded by the alleged root reality discussed below.

If $b^2 - ac = 0$, σ_1 and σ_2 coincide so the two branch tangents would coalesce. This is bizarre to say the least, but could happen.

§33.5.4. Are the Roots Always Real?

Intuitively it appears that the two roots of (33.21) must be real. The argument goes as follows: one of the two branches is supposed to exist since by stipulation B has been located while traversing an actual equilibrium path. Its tangent at B must therefore correspond to one of the roots of (33.21). If this argument is accepted, one one of the roots is real; whence the other one must also be real because a, b and c are real coefficients.

This indirect "proof" is not intellectually satisfying, especially to a mathematician. It would be preferable to prove the root reality by direct reasoning concluding that $b^2 - ac \geq 0$. However the writer has not been able to find such a proof in the literature, and personal efforts (a couple of hours trying) have been so far unrewarding.

§33.6. Multiple Bifurcation Points

If the bifurcation point at B is multiple,[4] meaning that the rank deficiency of $\mathbf{K}$ therein exceeds one, the branching analysis gets more considerably more complicated. Suppose that the multiplicity is m. Then the null subspace of $\mathbf{K}$ at B can be always be spanned by m independent orthonormalized eigenvectors $\mathbf{z}_i$, $i = 1, 2 \ldots m$.[5]

The state decomposition at B is appropriately generalized by expressing $\dot{\mathbf{u}}$ at B in terms of the particular solution $\mathbf{y}$, and the m null space basis vectors $\mathbf{z}_i$. The latter must be scaled by m amplitude coefficients. Substitution into the second-order rate equations yield a system of m quadratic equations in the $\mathbf{z}_i$ amplitudes. If none of these degenerate, Bezout's theorem says that we will get 2^m roots. Which shows that the number of equilibrium branches passing through B may be expected to grow up exponentially with the multiplicity: 4 for $m = 2$, 8 for $m = 3$, etc. The question of real versus complex roots, however, comes back with a vengeance.

[4] Some authors, e.g., Thompson and Hunt [769] identify critical points with rank deficiency exceeding one as *compound*. They state: "a compound critical point can be viewed as two or more coincident critical points." If the rank deficiency is one, they call the critical point *distinct*.

[5] The existence of this fully spanned subspace is guaranteed in the conservative case because $\mathbf{K}$ is real symmetric.

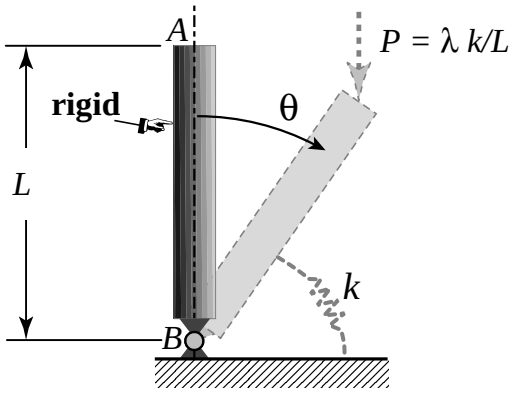

FIGURE 33.5. The hinged rigid cantilever under a vertical load. The structure can only move in the plane of the figure.

§33.7. The Hinged Rigid Cantilever

Levels 1 through 3 of bifurcation analysis are illustrated on the hinged rigid cantilever problem depicted in Figure 33.5. A *rigid* strut of length L and supported by a torsional spring of stiffness k, is axially loaded by a force $P = \lambda P_{ref}$ with $P_{ref} = k/L$, which remains vertical. The structure can only move in the plane of the figure. Note that k has the physical dimension of force $\times$ length, *i.e.* of a moment. Hence the definition $P = \lambda k/L$ renders λ dimensionless.

As just noted, the dimensionless stage control parameter is $\lambda = P\,L/k$. As state parameter we pick the tilt angle θ (radians) as most appropriate for hand analysis. The total potential energy is

$$\Pi = U - W = \tfrac{1}{2}k\theta^2 - P\,u = \tfrac{1}{2}k\theta^2 - PL(1-\cos\theta) = k\left[\tfrac{1}{2}\theta^2 - \lambda(1-\cos\theta\right]. \tag{33.24}$$

in which $u = L(1-\cos\theta)$ is the downward displacement of the load. The equilibrium equation in terms of θ is

$$r = \frac{\partial\Pi}{\partial\theta} = k(\theta - \lambda\sin\theta) = 0, \tag{33.25}$$

which may be readily verified with a Free Body Diagram (FBD). This equation has the two solutions

$$\theta = 0, \qquad \lambda = \frac{\theta}{\sin\theta}. \tag{33.26}$$

These pertain to the primary (vertical or untilted) and secondary (tilted) equilibrium paths, respectively. The two paths intersect at $\lambda = 1$, which is therefore a bifurcation point.

§33.7.1. Finding the Critical Point

The first-order rate (incremental) equation in terms of θ is

$$K\dot{\theta} - q\dot{\lambda} = 0, \tag{33.27}$$

in which

$$K = \frac{\partial r}{\partial\theta} = k(1-\lambda\cos\theta), \qquad q = -\frac{\partial r}{\partial\lambda} = k\sin\theta. \tag{33.28}$$

On the primary path, $\theta = 0$, the stiffness coefficient K vanishes at

$$\lambda = \lambda_{cr} = 1, \qquad \text{or} \quad P = P_{cr} = k/L. \tag{33.29}$$

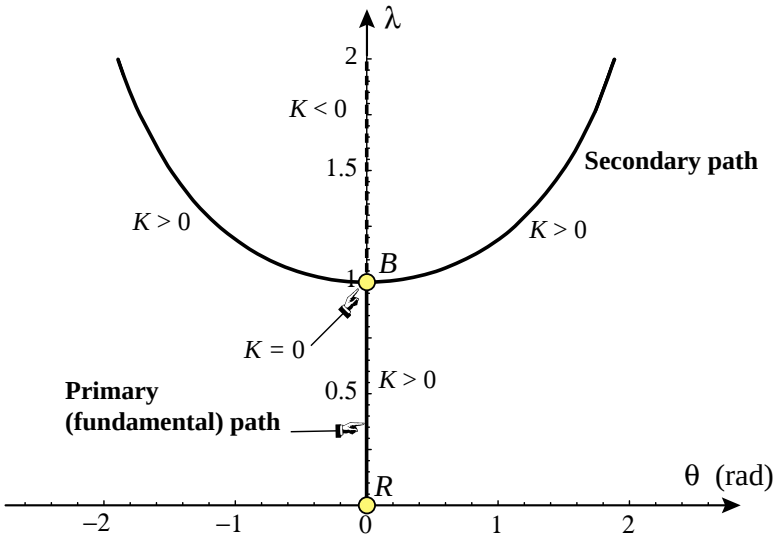

FIGURE 33.6. The sign of the stiffness coefficient K for the hinged cantilever response.

Over the primary path K is positive (negative) if $\lambda < 1$ ($\lambda > 1$), respectively. For the secondary path, which is $\lambda = \theta/\sin\theta$, the stiffness is given by

$$K = k\left(1 - \frac{\theta\cos\theta}{\sin\theta}\right), \tag{33.30}$$

which vanishes at $\theta = 0$ because $\theta/\sin\theta \to 1$ as $\theta \to 0$. If $\theta \neq 0$, $K > 0$. The five cases as regards the sign of K are summarized in Figure 33.6. Because K is a scalar, positive and negative values corresponds to stable and unstable equilibrium, respectively, with neutral stability at B. Stable (unstable) paths are drawn with full (dashed) lines.

It is seen that $\theta = 0^\circ$ and $\lambda = 1$ is the only point at which K vanishes, and consequently is the only critical point. Let us verify now that it is a bifurcation point. Since the system has only one degree of freedom (DOF), the unit-length-normalized null eigenvector is simply the scalar $z = 1$. The inner product $\mathbf{q}^T\mathbf{z}$ reduces to

$$qz = q = k\sin\theta, \tag{33.31}$$

which vanishes at $\theta = 0^\circ$. Hence ($\lambda_{cr} = 1$, $\theta_{cr} = 0^\circ$) is a bifurcation point, labelled B in the figures.

§33.7.2. Branching Analysis

In this problem the particular solution $\mathbf{y}$ vanishes because there is only one DOF. We may therefore take

$$\dot\theta = \sigma\mathbf{z}\dot\lambda = \sigma,\dot\lambda \tag{33.32}$$

as state decomposition at B. The second-order rate equation is

$$\lambda\sin\theta\,\dot\theta\dot\theta - 2\cos\theta\,\dot\theta\dot\lambda = 0, \tag{33.33}$$

Upon substituting $\dot\theta = \sigma\dot\lambda$, (33.33) yields the quadratic equation (33.21), with $a = \lambda\sin\theta$, $b = -2$, $c = 0$. At the bifurcation point ($\lambda = 1$, $\theta = 0$) we get

$$0.\sigma^2 - 2\sigma = -2\sigma = 0 \tag{33.34}$$

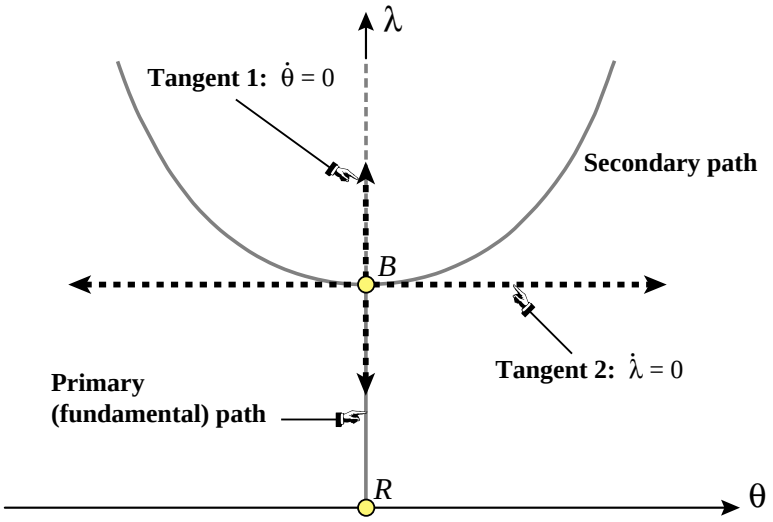

FIGURE 33.7. The two branch directions at the bifurcation point B of the hinged cantilever.

The two roots of (33.34) viewed as a degenerate quadratic equation are

$$\sigma_1 = 0, \qquad \sigma_2 = \infty, \tag{33.35}$$

which lead to the branching solutions

$$\dot{\theta} = 0, \qquad \dot{\lambda} = 0. \tag{33.36}$$

These branches are the tangents to the primary (vertical bar) and secondary (tilted bar), respectively, at the bifurcation point. See Figure 33.7.

This Figure also shows the post-buckling response, which for this problem is easily obtained from the exact equilibrium solutions (33.26). According to the qualitative classification of Chapter 29, the bifurcation point is of stable-symmetric type. The subclassification of a symmetric bifurcation point into stable and unstable cannot be discerned, however, from the level-3 branch-tangent analysis carried out above, because it requires level-4 information on the *curvature* of the **z**-directed branch.

§33.8. The Inclined Spring Propped Rigid Cantilever

To illustrate the occurrence of asymmetric buckling we consider a variant of the previous example, depicted in Figure 33.8. A *rigid* strut AB of length L is hinged at the base and loaded by a vertical load P at the top B. The strut can only move in the plane of the figure. The structure is stabilized by an inclined extensional spring of stiffness k. The spring direction forms a angle $0 \le \varphi \le 90^\circ$ with the ground, which is called the *rise angle*. The attachment point C remains fixed as the strut top moves. The applied force is parametrized as $P = \lambda\, k\, L$, in which the control parameter λ is dimensionless.

Since the strut is rigid, the system has only one degree of freedom (DOF). Two convenient choices are marked in red in Figure 33.8(b): the horizontal top displacement u (positive to the left) and the tilt angle θ (positive CW). They are linked by $u = L\sin\theta$. We pick the the tilt angle.

The original spring length BC is $L_{s0} = L/\cos\varphi$. If the strut tilts by θ, the deformed spring length can be obtained by applying the cosine law to triangle BCA', which gives $L_{sd}^2 = L^2(1 + \cot\varphi^2 + 2\cot\varphi * \sin\theta)$. The elongation is

$$\delta = L_{s0} - L_{s0} = L\,(\sqrt{\csc\varphi^2 + 2\cot\varphi\ \sin\theta} - \csc\varphi). \tag{33.37}$$

This function is not symmetric with respect to θ, a feature that will trigger asymmetyric buckling.

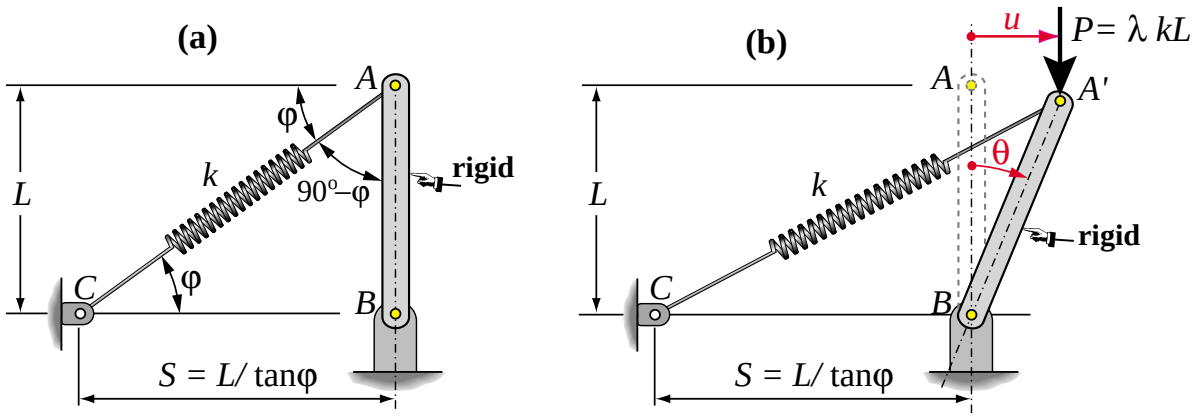

FIGURE 33.8. A rigid cantilever propped by an inclined spring.

§33.8.1. Critical Point Analysis

The total potential energy (TPE) as function of θ is $\Pi = U - W$, in which

$$U = \tfrac{1}{2} k\,\delta^2, \quad W = P\,L(1-\cos\theta) = \lambda\,k\,L^2(1-\cos\theta). \tag{33.38}$$

We will employ the dimensionless TPE $\tilde{\Pi}$ obtained on didiving through by kL^2. This is a function of φ, θ and λ alone:

$$\tilde{\Pi} = \tfrac{1}{2}\left[\sqrt{\csc\varphi^2 + 2\cot\varphi\,\sin\theta} - \csc\varphi\right]^2 - \lambda\,k\,L^2(1-\cos\theta). \tag{33.39}$$

The associated dimensionless residual is

$$r = \frac{\partial\tilde{\Pi}}{\partial\theta} = \cot\varphi\,\cos\theta\left(1 - \frac{1}{\sqrt{1+\sin(2\varphi)\,\sin\theta]}}\right) - \lambda\,\sin\theta. \tag{33.40}$$

As usual, $r = 0$ has two equilibrtium path solutions:

$$\theta = 0, \qquad \lambda_s = \cot\varphi\,\cot\theta\left(1 - \frac{1}{\sqrt{1+\sin(2\varphi)\,\sin\theta}}\right). \tag{33.41}$$

The first one is the equation of the primary path, which corresponds to the untilted column. The second one represents the secondary path. To find their intersection is it convenent to Taylor expand the secondary path about $\theta = 0$:

$$\lambda_s = \cos\varphi^2 - \frac{3\,\theta}{4}\,\cos^2\varphi\,\sin(2\varphi) - \frac{\theta^2}{16}\left[3\,\cos^2\varphi^2 + 5\,\cos^2\varphi\,\cos(4\varphi)\right] + \ldots \tag{33.42}$$

Making $\theta \to 0$ yields the critical λ at the intersection of (33.41), thus giving the bifurfaction point as function of the rise angle:

$$\lambda_{cr} = \cos^2\varphi. \tag{33.43}$$

Thus reducing the rise angle increases the critical load, at the cost of increasing the distance $S = L/\tan\varphi$. If $\varphi \to 0$, $\lambda_{cr} \to 1$, which was previously obtained for the propped rigid cantilever in §5.6.2.

A set of control-state response plots for specific rise angles is shown in Figure 33.9. The asymmetric nature of the bifurcation is evident from the diagrams. The structure will favor buckling to the right, for which $\theta > 0$. If the column is made to tilt left, it would go through a limit point except for a special angle noted next.

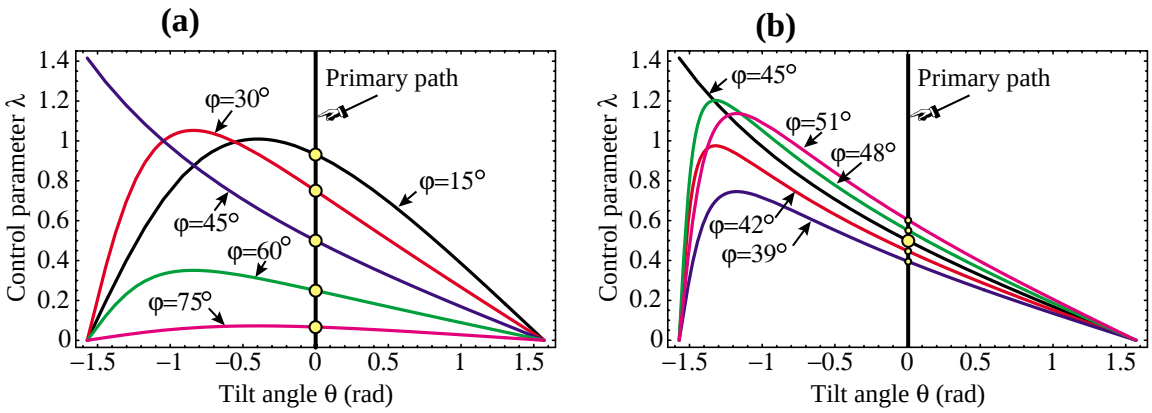

FIGURE 33.9. Equilibrium paths of the propped rigid cantilever with inclined spring: (a) load versus tilt angle responses for rise angles φ of 15°, 30°, 45°, 60°, and 75°; (b) responses in the vicinity of $\varphi = 45°$, showing an interesting shape transition.

Notice that the response for $\varphi = 45°$ in Figure 33.9(a) has a different shape than the others in that it does not display a limit point for $\theta < 0$. This anomaly is explored in Figure 33.9(b), which plots responses in the vicinity of that angle. Physical reason for the outlier shape: if $\theta \to -90° = -\frac{1}{2}\pi$, the strut top B coalesces with C, reducing the spring length to zero.

§33.8.2. Stiffness Analysis

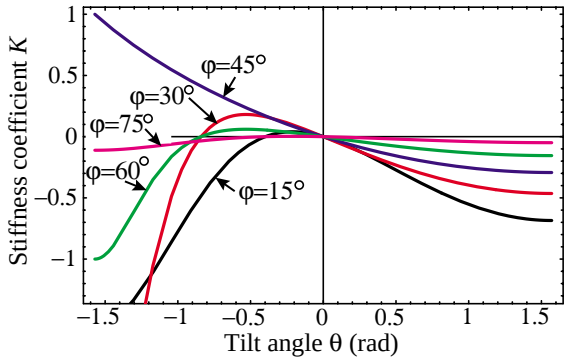

FIGURE 33.10. Variation of stiffness coefficient K over secondary path for the same set of rise angles as in Figure 33.9(a).

The tangent stiffness coefficient along the secondary path is given by[6]

$$K_s = \left.\frac{\partial r}{\partial \theta}\right|_{\lambda->\lambda_s} = \tfrac{1}{2}\cot\varphi\left(\frac{2\csc\theta + \frac{1}{2}\left[5+\cos(2\theta)\right]\sin(2\varphi)}{[1+\sin\theta\sin(2\varphi)]^{3/2}} - \csc\theta\right) \tag{33.44}$$

This is plotted in Figure 33.10 for the sample rise angles shown in Figure 33.9(a). As can be seen $K < 0$ if $\theta > 0$, which confirms that the bifurcation point is unstable for $\varphi > 0$, whence the column buckles to the right.

Additional analysis of this problem are posed as Exercises.

[6] Direct differentiation of r leads to an unwieldy result. The fairly compact expression (33.44) was obtained by the `FullSimplify` function of *Mathematica* after making appropriate assumptions on φ and θ, and doing some crunching.

Homework Assignments for Chapter 33
Nonlinear Bifurcation Analysis

EXERCISE 33.1 [A:10] Consider the symbols introduced in (33.9) for the second-order rate equation $\ddot{\mathbf{r}} = \mathbf{0}$:

$$\mathbf{L} = \frac{\partial \mathbf{K}}{\partial \mathbf{u}}, \qquad \mathbf{N} = \frac{\partial \mathbf{K}}{\partial \lambda} = -\frac{\partial \mathbf{q}}{\partial \mathbf{u}}, \qquad \mathbf{h} = \frac{\partial \mathbf{q}}{\partial \lambda}. \tag{E33.1}$$

(Here $\mathbf{L}$ is a "cubic" matrix, $\mathbf{N}$ an ordinary matrix, $\mathbf{h}$ a vector.) Are these relations true? (Show work, be careful checking signs.)

EXERCISE 33.2 [A:20] If $a \to 0$ in the quadratic equation (33.21) while $b \neq 0$, one of the roots, say σ_1, goes to ∞ whereas the other one becomes $\sigma_2 = -c/2b$. This condition defines a *symmetric* bifurcation. Show that in such a case the branch direction corresponding to σ_1 coincides with the buckling mode $\mathbf{z}$, and draw a bifurcation diagram similar to Figure 33.1.

EXERCISE 33.3 [A:40] Algebraically prove that the roots of the quadratic equation (33.21) are real[7]

EXERCISE 33.4 [A:20] The LPB first order rate equations are $\dot{\mathbf{r}} = \mathbf{K}\dot{\mathbf{u}} - \mathbf{q}\dot{\lambda} = \mathbf{0}$, in which $\mathbf{K} = \mathbf{K}_0 + \lambda \mathbf{K}_1$ and where $\mathbf{K}_0$, $\mathbf{K}_1$ and $\mathbf{q}$ are constant. By working out for this case the quadratic equation (33.21) with coefficients defined by (33.22) show that LPB can only predict *symmetric bifurcation*.[8] (*Hint*: use (E33.1) to show that $\mathbf{L} = \partial \mathbf{K}/\partial \mathbf{u} = \mathbf{0}$, $\mathbf{N} = \partial \mathbf{K}/\partial \lambda = \mathbf{K}_1$, $\mathbf{h} = \partial \mathbf{q}/\partial \lambda = \mathbf{0}$, and then apply the result of Exercise 33.2 to show that one root goes to ∞ while the other one remains finite.) What wonderful thing happens if $\mathbf{K}_1\,\mathbf{y} = \mathbf{0}$?

EXERCISE 33.5 [A:20] The *propped cantilever* shown in Figure 5.5 of Chapter 5 consists of a *rigid* bar of length L pinned at A and supported by a linear extensional spring of stiffness k at the top. The spring is assumed to be capable of resisting both tension and compression and retains its horizontal orientation as the system deflects. The bar may rotate all the way around the pin. The rigid bar is subjected to a vertical dead load P that remains vertical. Define dimensionless control and state parameters as

$$\lambda = \frac{P}{kL}, \qquad \mu = \sin\theta. \tag{E33.2}$$

Analyze the stability of the propped cantilever in a manner similar to that done for the hinged cantilever in §33.7. Show that the secondary equilibrium path is the circle $\lambda^2 + \mu^2 = 1$ and sketch the response paths showing the complete circle. From this diagram, can you tell whether the bifurcation point at $\lambda = 1$ is stable-symmetric or unstable-symmetric? How about the one at $\lambda = -1$?

EXERCISE 33.6 [A:15] A very simple exercise in optimal stability design. Consider the hinged rigid cantilever propped by an inclined spring, studied in §33.8. Assume that the spring pictured in Figure 33.8 is actually a taut guy cable of modulus E_c, cross-section area A_c and length $L_c = L/\sin\varphi$. The equivalent spring stiffness is $k_c = E_c\,A_c/L_c$. The only design variable is the rise angle φ. As per (33.43), the critical load is $P_{cr} = k_c\,L\,\cos^2\varphi$. Show that the angle φ_{best} that maximizes P_{cr} is roughly 35 degrees.[9]

---

[7] A very difficult assignment worth of a journal paper. I am not aware of anybody that has done it for the general case.

[8] No textbook on stability tells you about this important modeling restriction. Be proud to be the first to prove it.

[9] Of course that result assumes that the column buckles to the right, since a cable cannot take compression. In practice it would be better to put *two* symmetrically arranged cables.